SEARCH FOR CARBONATES ON MARS WITH THE OMEGA / MARS EXPRESS DATA. D. Jouglet[1], F. Poulet[1], J.P. Bibring[1], Y. Langevin[1], B. Gondet[1]. [1]IAS, Université Paris-Sud, 91495 Orsay Cedex, France, denis.jouglet@ias.fr.

Introduction: Key minerals for the study of the past of Mars, such as phyllosilicates, sulfates or hydroxides, have been discovered by the Mars Express / OMEGA experiment [e.g. 1,2]. This abstract focuses on the search for carbonates from the OMEGA dataset. The presence or the lack of carbonates on the Martian surface is very important to 1) better understand the climatic and geological past of the planet, since carbonates easily form in aqueous media; 2) get new elements about the evolution of a primitive thicker CO_2 atmosphere, since dissolved carbon dioxide precipitates in carbonate minerals. Moreover the carbonate formation is also largely favored by biological processes.

Several Martian missions have tried unsuccessfully to detect carbonate minerals on the surface of Mars, either orbital instruments like IRS [3] or TES [4], or landers and rovers up to now. TES detected what can be interpreted as carbonates in the Martian dust but only in small amounts [5]. SNC meteorites, assumed to originate from the Martian surface, present carbonate inclusions [e.g. 6]. Several scenarios have been proposed to explain this lack of carbonate in the Martian observations, from the chemical conditions to inhibit carbonate formation [7] to their UV photolysis if they were ever formed [8].

The OMEGA investigation, on board the ESA Mars Express mission, has been mapping Mars surface by means of visible-infrared hyperspectral reflectance imagery at a 0.3- to 5-kilometer resolution since December 2003. In the near-infrared all kinds of carbonate minerals exhibit two strong absorption bands at 3.4 and 3.9 µm. This abstract presents the detection method based on these bands and its results.

Detection tool: Carbonate minerals are formed by the precipitation of dissolved CO_2 with different cations, forming calcite ($CaCO_3$), siderite ($FeCO_3$), dolomite ($CaMg(CO_3)_2$) or other minerals. The near-infrared reflectance spectra of all these carbonate minerals present several specific absorption features in the OMEGA wavelength range (Fig. 1). Of particular interest are the two strong absorptions at 3.4 and 3.9 µm (Fig. 1). Here, we focus on the detection of the 3.4 µm band because the instrumental non-linearities in the 3.9 µm spectral region precludes the fine measurement of the 3.9 µm band depth without an improved knowledge of the instrument behavior.

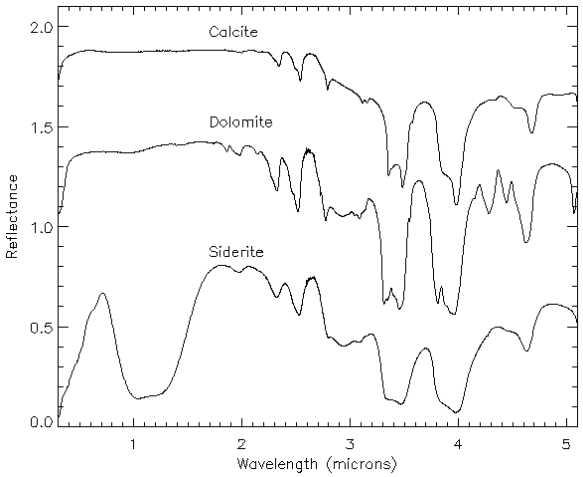

Figure 1 : Near-infrared albedo spectra of several carbonate minerals (from RELAB./Brown University). Calcite is shifted vertically by 1.0, Dolomite by 0.5 and Siderite is not shifted. These three carbonate minerals exhibit two strong absorption bands at 3.4 and 3.9 µm.

Considering the number of OMEGA spectra to test (several hundreds of millions), a tool has been developed to evaluate the 3.4 µm carbonate band automatically and efficiently. The automatic process for carbonate detection first converts the OMEGA raw data to radiance spectra of the surface. These spectra are then corrected for atmospheric absorptions and converted to albedo spectra, thanks to the knowledge of the solar insulation and the estimation of the surface thermal emission [9]. Every OMEGA albedo spectrum exhibits a broad hydration band centered on 3 µm [9]. Since the 3.4 µm carbonate band is inside this broad band, usual band assessment tools like band depth versus a linear continuum cannot be efficiently used here. We decided therefore to derive the continuum of each OMEGA spectrum thanks to a polynomial interpolation between the ranges [3.15 – 3.30 µm] and [3.57 – 3.74 µm]. The automatic process subtracts the derived continuum from the albedo spectra and the 3.4 µm band depth is calculated with the following formula:

$$Band\_Depth = 1 - mean(Albedo(3.38 : 3.46 \mu m))$$

The mean is constructed on five spectels. This method has been tested on laboratory spectra (Fig. 2). For albedo spectra of mixtures composed of palagonite (hydrated Martian analog) with 1%, 5% and 20% of carbonate, the calculated band depths are respectively of 0.31%, 0.60% and 2.62%.

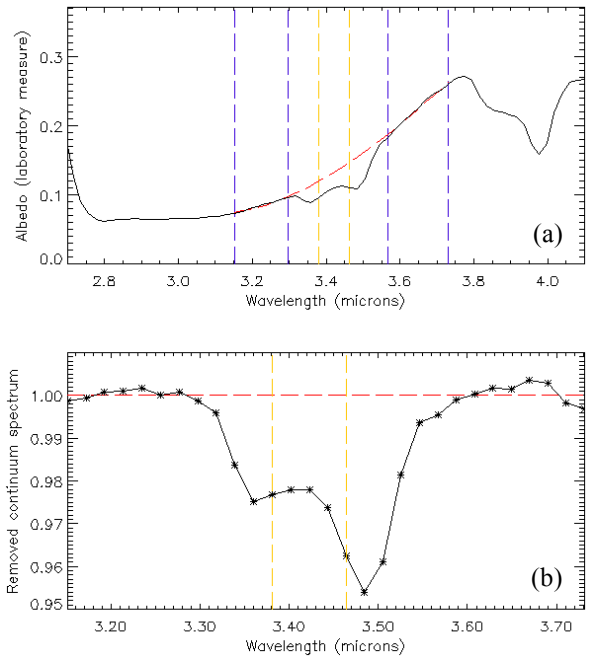

Figure 2 : Application of the 3.4 µm carbonate detection tool on a laboratory spectrum obtained during the ground calibration of OMEGA. The blue dashed lines borders the areas used for polynomial fitting, the yellow dashed lines the area used for band depth calculation. (a) Black: radiance spectrum of a 80% palagonite / 20 % calcite mixture divided by a reference radiance spectrum (MgO), so as to get the albedo spectrum. Red: polynomial interpolation to simulate the spectrum continuum at 3.4 µm. (b) Albedo spectrum on which the continuum was subtracted and from which the 3.4 µm band depth is evaluated.

This tool is first applied on a few regions known to exhibit hydrated minerals. Then a large part of the dataset is automatically processed with adapted selection criteria, which are discussed in the next sections.

Hydrated mineral areas: A few regions rich in hydrated minerals have been discovered by OMEGA, for example Mawrth Vallis with phyllosilicate outcrops [2] or Terra Meridiani with sulfates [10]. These areas are known to form very early in Mars history in a wet environment. In particular the formation conditions of clays were quite similar to what is needed to form carbonates. The carbonate detection tool is first applied to such regions, but no enhancement of the band depth can be detected there. The OMEGA pixels where hydrated minerals are detected do not exhibit any carbonate feature.

Global search: The 3.4 µm carbonate detection method is applied on all OMEGA spectra for the orbits 30 to 1989. This corresponds to 140 million albedo spectra, covering about 80% of the Martian surface between 80°N and 80°S. After orbit 1989 new instrumental evolutions appear, which will lead us to adapt our automatic detection tool in the future. The global search is divided into three steps: 1) a general search so as to determine which factors are responsible for wrong detections; 2) an automatic selection of potential carbonate spectra thanks to a restriction of the influence of these factors; 3) an eye visualization of the candidates.

Influence of ice and noise. A first study of the carbonate detection has revealed that two major factors are responsible for false-positives: the presence of water ice and a low signal to noise ratio.

Water ice is responsible for a strong and broad absorption band from 3.0 to 3.4 µm which can increase the 3.4 µm band depth measures. Every OMEGA spectra exhibiting water ice features have therefore to be ignored to avoid wrong detections. Water ice can be also detected by the presence of a 1.5 µm absorption band. However, this band is subject to a non-linearity of the instrument that may create a small band without the presence of ice. A correction curve is applied to improve the water ice detection level [11]. Taking into account the small variations due to noise, we consider that all spectra exhibiting a 1.5 µm band greater than about 1% could be due to the presence of water ice. The influence of the presence of water ice on the 3.4 µm band depth is presented in Fig. 3 for a fraction of the OMEGA dataset with a 1.5 µm band depth up to 2%. We notice that the 3.4 µm band depth increases with the water ice criterion as well as the number of detections. The distribution presents a small peak around 0%, corresponding to the majority of the dataset which is not contaminated by water ice. The upper limit of the peak is about 1%, corresponding to the small variations due to noise. We decide to fix this value as the limit beyond which spectra are removed from the global study. This excludes the majority of the water ice spectra without losing non icy spectra. We recall that the albedo spectra presenting a 1.5 µm feature between 0% and 1% may be either actual water ice or just slight noise.

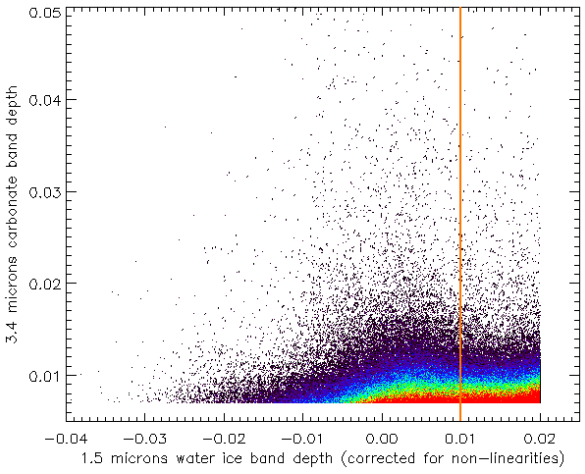

Figure 3 : Correlation between the 3.4 µm carbonate band depth and the 1.5 µm water ice band depth (corrected for instrumental non linearities). The dataset tested is made of 150,000 spectra (3.4 band depth > 0.007, 3.7 µm flux > 60 DN and 1.5 µm band depth < 2%). The rainbow color code illustrates the density of data. The orange line is the final selection criterion.

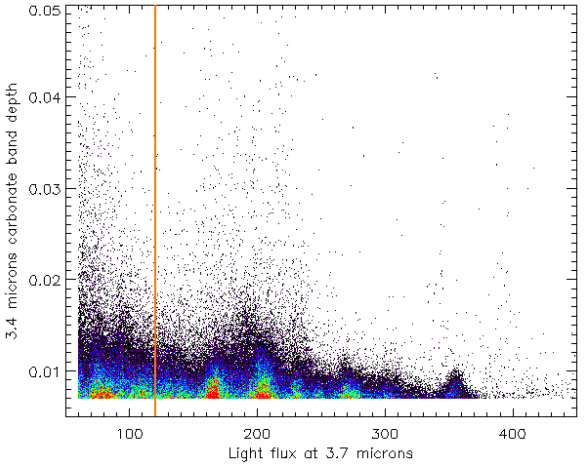

Figure 4 : Correlation between the 3.4 µm carbonate band depth and the received flux at 3.7 µm. Low signal to noise ratio can be responsible for increased 3.4 µm features. The dataset tested is made of 150,000 spectra (3.4 band depths > 0.007, 3.7 µm flux > 60 DN and 1.5 µm band depth < 2%). The rainbow color code illustrates the density of data. The orange line is the final selection criterion.

The second factor that can influence the value of the 3.4 µm band depth is noise. When the light flux received in the [2.5 - 5.1 µm] range tends to zero, the signal to noise ratio dramatically decreases. In some random cases noise can create a higher value of the 3.4 µm carbonate band and be responsible for false positives not related to the presence of carbonates. Fig. 4 presents the correlation of the 3.4 µm band depth with the received flux for a fraction of the dataset with a light flux of at least 60 DN. Under this value the signal to noise ratio of spectra is too low and precludes us to efficiently assess the presence of a band. The flux is measured at 3.7 µm, which is approximately the end of the 3 µm broad hydration band. The figure confirms that when the flux reduces, the 3.4 µm band depth slightly increases as well as the number of detections. We choose to remove every spectrum with a 3.7 µm flux lower than 120 DN to avoid these wrong detections and keep the most opportune cases.

Automatic detections. As discussed, the final thresholds selected for the global automatic detection study are: a 3.7 µm flux greater than 120 DN and a 1.5 µm water ice band depth lower than 1%. Fig. 3 and 4 show that to avoid the highest densities in the distribution and to restrict to the most opportune cases, only pixels exhibiting a 3.4 µm carbonate band depth greater than 1% are kept in the global study. Numerical simulations from laboratory measurements showed that it represents approximately 10% weight of carbonate in a mixture with palagonite. Finally a geographical criterion is added to the automatic detection tool: a detection is recorded only if at least another detection is present in its neighborhood of 35 pixels. This considers that a carbonate mineralogical unit would be present on more than only one pixel, and this excludes a large number of wrong detections due to instrumental defects. With these criteria the automatic tool obtained around 4,000 detections. This value is very low compared to the size of the dataset.

Manual diagnostic of the detections: Each of these 4,000 detections requires an eye visualization to perform the carbonate diagnostic. A large part of these detections is attributed to the presence of water ice, with a 1.5 µm band depth value between 0% and 1%. Another part is attributed to noise or instrumental defects. Amongst the remaining detected spectra no obvious carbonate-like spectra can be detected, but only small features that deserve careful analysis. For each of these cases a study is lead on the region with all the OMEGA data observing them. A few examples are presented here.

A first example is located in the region around 129°E 67°N, detected in the OMEGA orbit 1059. A spectrum is given on Fig. 5, for a 3.4 µm band depth of 1.2%. We can see that between 3.3 µm and 3.5 µm the shape of the spectrum is quite similar to that of the carbonate examples. No water ice features can be detected, and this 3.4 µm band is greater than noise. The 3.4 µm band depth of this orbit is mapped on Fig. 6. A strong spatial grouping of the 3.4 µm band enhancement is observed in this area. The OMEGA orbit 1037

reveals a same grouping at the same location, but the other OMEGA orbits observing this area reveal nothing there. No other carbonate feature such as the 2.35, 2.55 or 3.9 µm bands can be detected in the corresponding spectra. It is therefore difficult to conclude about the presence of carbonate in this place.

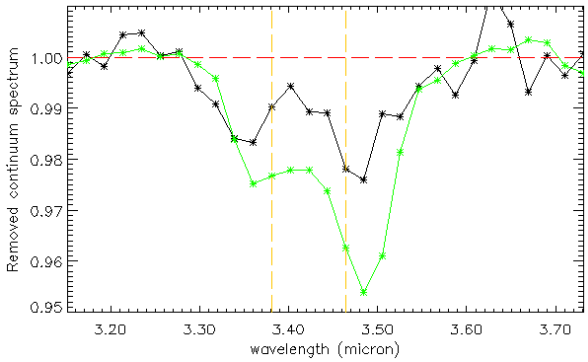

Figure 5 : Black curve: Continuum-removed albedo spectra around the 3.4 µm carbonate band of the point 129°E 67°N (from OMEGA orbit 1059). Green curve: for comparison, continuum-removed albedo spectra of a laboratory-measured carbonate.

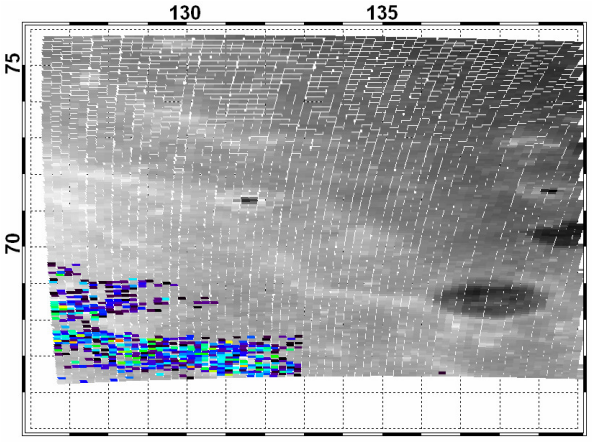

Figure 6 : Map of the 3.4 µm carbonate band depth of the OMEGA orbit 1059 over the MOLA altimetry. The color scale (rainbow) ranges between 0% and 2%.

A second example is located in the region around 70°E 77°N, detected in the OMEGA orbit 1001 (Fig. 7). An enhancement of the 3.4 µm carbonate band is detected for a very localized area. A following orbit, the 1012, also shows a slight increase of the 3.4 µm carbonate feature but around this area. No particular enhancement is observed by the other OMEGA orbits observing this area. This could support the presence of carbonates in moving materials, for example clouds in atmosphere or dust on the surface. Moreover these two observations are linked to slight variations of albedo.

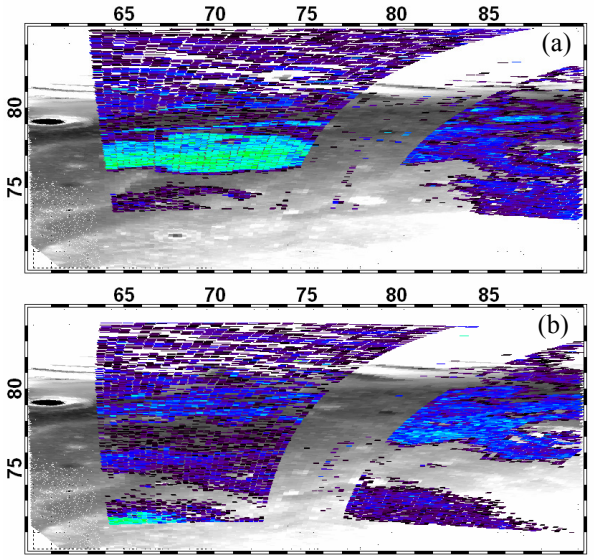

Figure 7 : Map of the 3.4 carbonate band depth of the OMEGA orbits 1001 (a) and 1012 (b) over the MOLA altimetry. The color scale (rainbow) ranges between 0% and 2%.

Conclusion: The main conclusion of the search for carbonates on Mars with the OMEGA data is that no carbonate minerals can be detected on a global scale on Mars at the detection limit of this method. We do not even detect small localized areas of not ubiquitous carbonate minerals. The method presented here will be improved in the future with 1) the cross correlations between the 3.4 µm and the 3.9 µm carbonate features, and with 2) an 3.4 µm threshold dependent on the actual signal to noise ratio of each spectrum. We hope to reduce our detection limits with that way.

References: [1] Bibring J.-P. et al. (2005) *Science, 307,* 1576-1581. [2] Poulet F. et al. (2005) *Nature, 438*, 623-627. [3] Roush T. L. et al. (1986) *JGR, 102,* 1663-1670. [4] Stockstill K. R. et al. (2005) *JGR, 110,* CiteID E10004. [5] Bandfield J.L. et al. (2003) *Science, 301,* 1084-1087. [6] Jull A. J. T. et al. (1997) *JGR, 102,* 1663-1670. [7] Fonti S. et al. (2001) *JGR, 106,* 27,815-27,822. [8] Fairén A. G. et al. (2004) *Nature, 431,* 423-426. [9] Jouglet D. et al. (2007) *JGR,* in press. [10] Gendrin, A., et al. (2005), *Science*, 307, 1587– 1591. [11] Jouglet, D., et al. (2007), *this conference*.